Electronic Supplementary Material (ESI) for Nanoscale.

Supplementary Information for "p-type transition-metal doping of large-area MoS_2 thin films grown by chemical vapor deposition"

1. Optical micrograph and Raman spectra of MoS_2 films.

Figure S1 (a) shows an optical image taken on the Zn-doped MoS_2 film in the regime where two-terminal devices were fabricated (the sample was broken so the image was taken with two pieces put together). Raman measurements were conducted on the channel of each device. Figure S1 (b) and (c) are the spectra taken on the Zn-doped film and the undoped film, respectively. The separation between the A_{1g} and E^1_{2g} peaks is ~20 cm^{-1} in all these spectra, suggesting that the films are monolayer over an area of a few millimeters.

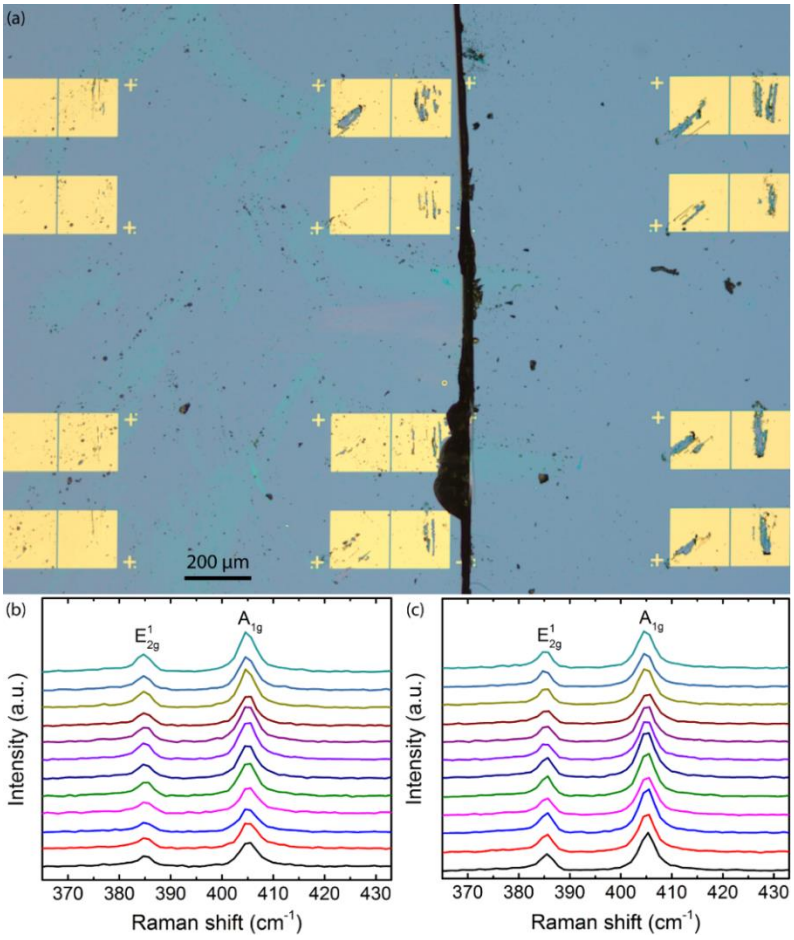

Figure S1. (a) Optical image of Zn-doped MoS_2 film. Particles exist in some regions, leading to color contrast. Raman spectra taken in the channel of each device on the (b) Zn-doped film and (c) undoped film. Different colors represent spectra taken at different spots.

2. Atomic Force Microscopy (AFM) scan of Zn-doped MoS_2 film

We scratched on the Zn-doped MoS_2 film and performed AFM measurement around the scratched area. As shown in Figure S2, the film thickness is ~ 0.7 nm, corresponding to a monolayer of MoS_2. We note that scratch may sometime enter the SiO_2 substrate, leading to a larger height across the edge.

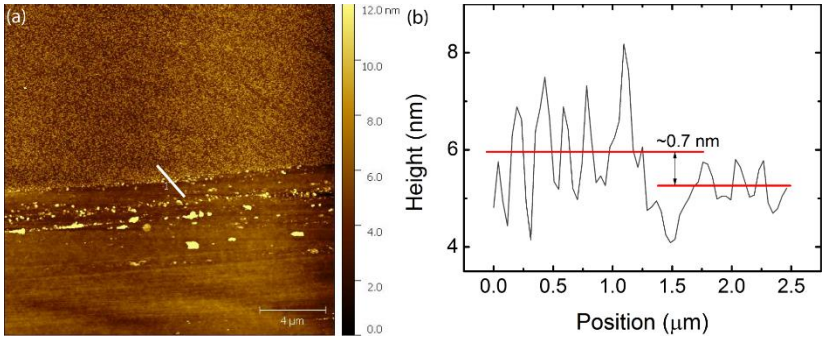

Figure S2. (a) AFM image of a Zn-doped MoS_2 film around a scratched area. (b) Height profile along the white line in (a).

3. XPS scan of Zn $2p_{3/2}$ core level of ZnO powder

X-ray photoelectron spectroscopy measurement was carried out on ZnO powder, as shown in Fig. S3. The binding energy of the Zn $2p_{3/2}$ peak is at ~1021.6 eV, which is lower than that in the Zn-MoS_2 film and ZnS powder, suggesting that residual oxygen is not significant in our film.

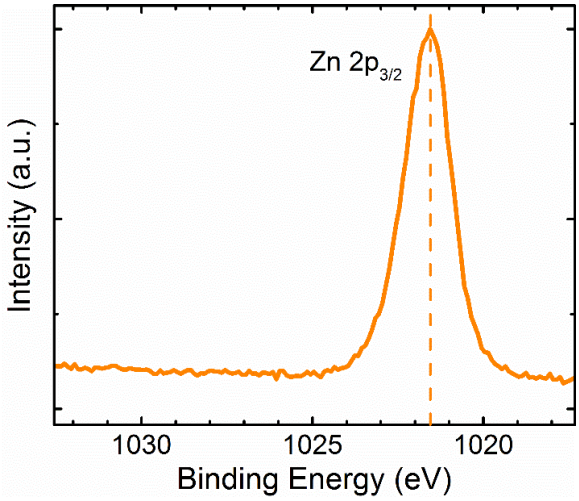

Figure S3. XPS scan of Zn $2p_{3/2}$ core level on ZnO powder.

4. XPS scan of O 1s core level of Zn-doped MoS_2 sample

XPS scan of O 1s core level was carried out on Zn-doped MoS_2, as shown in Figure S4. There is only a single peak at ~532.9 eV, which corresponds to O 1s peak from SiO_2 substrate.[1] This suggests that the amount of oxygen bounding with Zn is negligible compared with the oxygen in the substrate.

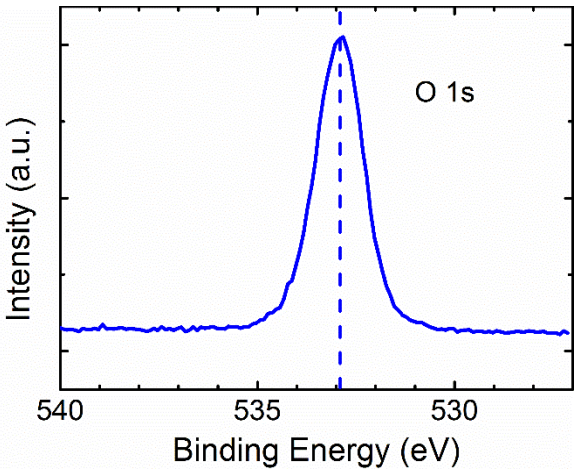

Figure S4. XPS scan of O 1s core level on Zn-doped MoS_2 sample.

5. Comparison of gate transfer curves before and after scratching

To confirm that the electrical properties measured on the devices without etching are mostly contributed from the channel area, we compared the gate transfer characteristics of a test device (Co-doped MoS_2) before and after the surrounding areas are scratched off. Figure S5 (a) shows the optical image after scratching and Figure S5 (b) is a comparison of gate transfer curves, which shows negligible changes.

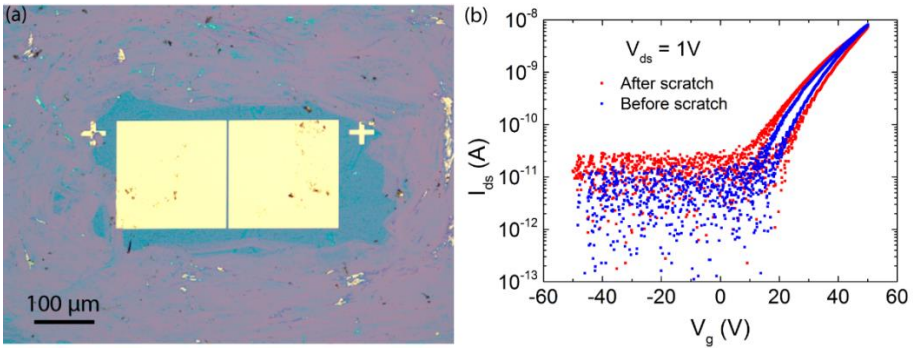

Figure S5. (a) Optical image of a test device after scratching. (b) Gate transfer characteristics before and after scratching.

6. Position dependence of Raman peak shift of Zn-doped MoS_2 films

Single acquisitions of Raman spectra were obtained on each device from Column 1 to Column 3 of the Zn-doped MoS_2 film (Figure S1). As the position of devices changes from right to left (from Column 3 to Column 1), both E^1_{2g} and A_{1g} peaks show a general trend of blue shift (Figure S6).

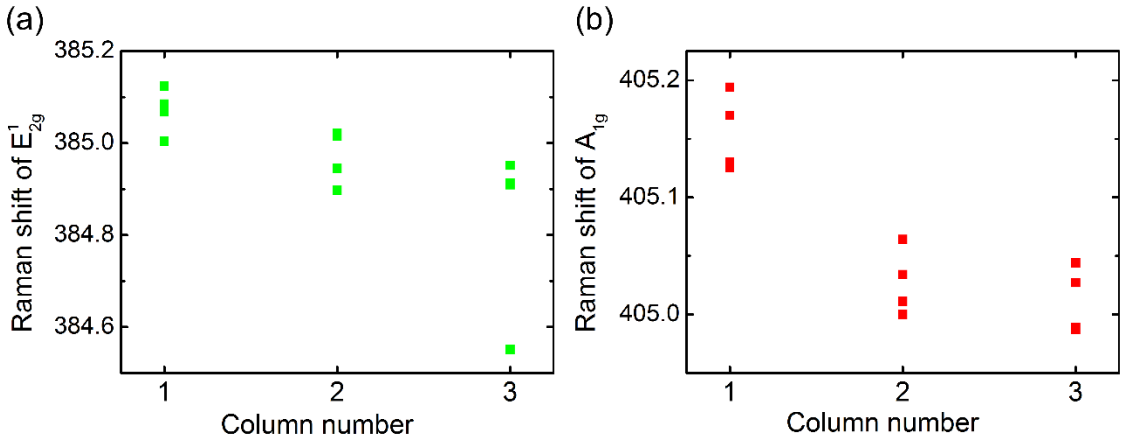

Figure S6. Raman peak position plots of (a) E^1_{2g} and (b) A_{1g} modes respectively obtained by single spectrum acquisitions from each device in the columns numbered from 1 to 3.

7. Raman characterization of film f3.

We carried out the growth of film f3, in which sulfur was introduced at a later time than film f2. The late exposure to sulfur leads to thicker deposition with both monolayer and bilayer regions, as identified by Raman spectroscopy (Figure S7).[2-4]

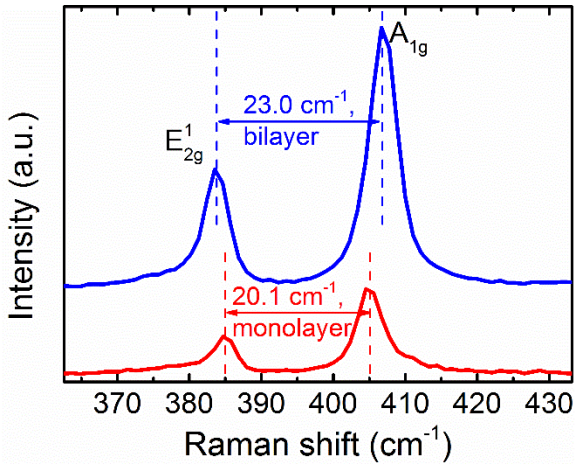

Figure S7. Two representative Raman spectra taken on film f3. The separation between A_{1g} and E^1_{2g} peaks are ~20 cm^{-1} and ~23 cm^{-1} for monolayer and bilayer films, respectively.

8. Gate transfer characteristics of a representative monolayer Zn-doped MoS_2 device (f2)

Figure S8 (a) shows a gate transfer curve of a monolayer Zn-MoS_2 device at the high gate bias region. Figure S8 (b) is the derivative of drain-source current with respect to gate voltage from -50 V to 50 V. It is clearly seen that the linear I_{ds}-V_g region is not reached, which prevents the determination of a threshold voltage using the conventional linear extrapolation method. Instead, we define the threshold voltage V'_{th} as the lowest gate voltage that is required to increase the drain-source current above the off state.

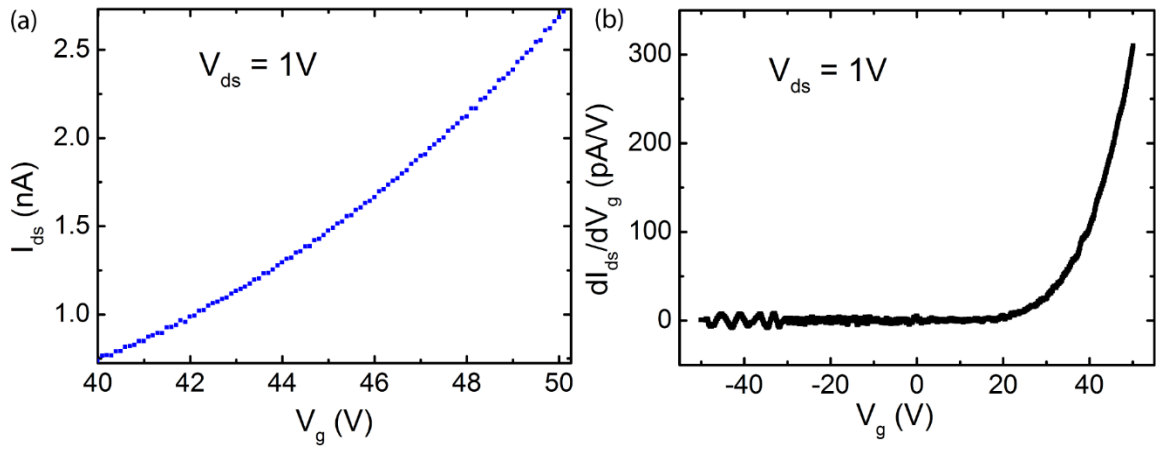

Figure S8. (a) Gate transfer curve of a Zn-doped MoS_2 devices. (b) The derivative of drain-source current with respect to gate voltage.

9. Gate transfer characteristics of films f4 and f5.

We further carried out two growths at a higher temperature (900 °C). The films are labeled as f4 and f5. The growth conditions for f4 and f5 are similar, except that the MoO_3 powder was placed ~1 inch away from the center of the furnace in the growth of f4, while it was placed right at the center in the growth of f5. Such high temperature growths lead to thicker deposition of bilayer films in addition to monolayer. Two terminal devices

were fabricated on these two films and their gate transfer characteristics before sulfur treatment are shown in Figure S9.

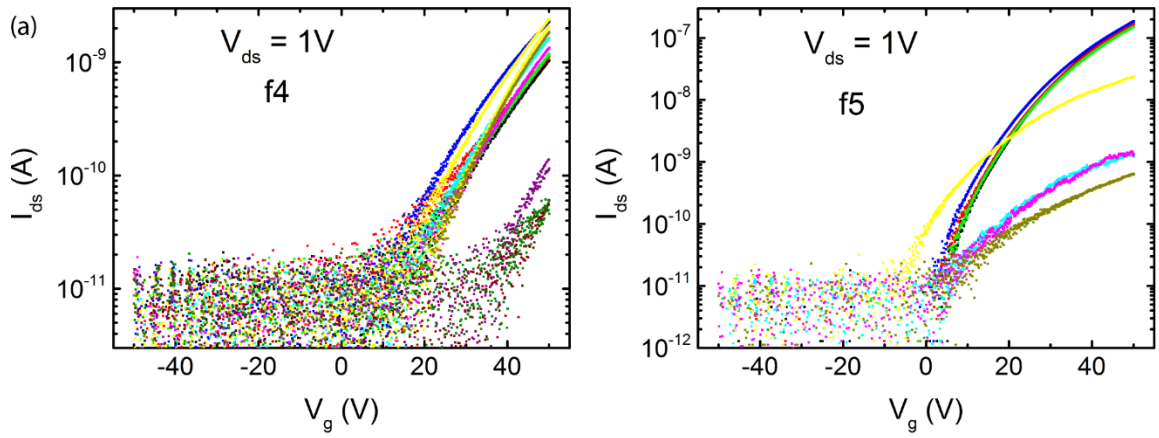

Figure S9. Gate transfer curves of two-terminal devices fabricated on films (a) f4 and (b) f5. Different colors represent different devices.

References

1 J. H. Kim, J. Lee, J. H. Kim, C. C. Hwang, C. Lee and J. Y. Park, *Applied Physics Letters*, 2015, **106**, 251606.

2 Y. Zhan, Z. Liu, S. Najmaei, P. M. Ajayan and J. Lou, *Small*, 2012, **8**, 966-971.

3 Y. Yu, C. Li, Y. Liu, L. Su, Y. Zhang and L. Cao, *Scientific reports*, 2013, **3**, 1866.

4 H. Schmidt, S. F. Wang, L. Q. Chu, M. Toh, R. Kumar, W. J. Zhao, A. H. C. Neto, J. Martin, S. Adam, B. Ozyilmaz and G. Eda, *Nano letters*, 2014, **14**, 1909-1913.